An EMC Susceptibility Study of Integrated Basic Bandgap Voltage Reference Cores

David KROLAK [1,2], Pavel HORSKY [2]

[1] Dept. of Radio Electronics, Brno University of Technology, Technická 12, 616 00 Brno, Czech Republic
[2] ON Design Czech s.r.o., onsemi company, Vídeňská 204/125, 619 00 Brno, Czech Republic

{David.Krolak, Pavel.Horsky}@onsemi.com

Submitted February 15, 2022 / Accepted July 25, 2022 / Online first August 16, 2022

Abstract. *This paper presents a comparative EMC susceptibility study of various integrated bandgap voltage reference cores. Conventional well-known bandgap references based on Kuijk, Brokaw and Tsividis concepts with reduced count of bipolar junction transistors in the core were analyzed. On top of the EMC susceptibility comparison, basic parameters like temperature drift, sensitivity to an operational amplifier input offset and line regulation are also discussed. The influence of a collector leakage current compensation at high temperatures is investigated as well.*

Keywords

Bandgap voltage reference, Brokaw, BCD, EMC, HF immunity, Kuijk, offset, temperature drift, Tsividis

1. Introduction

Many mixed-signal integrated circuits (ICs) require a built-in voltage reference generator, such as a bandgap voltage reference. This reference can be used for regulators, comparators, analog to digital converters (ADCs), digital to analog converters (DACs), bias current generators and for other blocks. The reference cell generates a constant DC voltage ideally independent on temperature, power supply, loading and manufacturing process variations.

Many articles focus on temperature dependence of voltage references usually within a limited temperature range from –50°C to 125°C [1–6]. With this temperature range, the reachable temperature coefficients (TCs) are tens of ppm/°C and even 2 ppm/°C with some more advanced techniques. But higher current consumption and higher supply voltage requirements are costs of these very low temperature variations [7]. In the automotive industry, the maximum junction temperature can go up to 200°C during operation. Voltage references designed to handle such high temperature are often using advanced curvature correction techniques based on measurement of temperature characteristic and using trimming [7], [8].

The automotive voltage references in sub-micron technologies are also limited by supply voltage where the reference has to be parametric, e.g. from 2 V to support fluctuating supplies [7]. The current consumption from this on-board power supply can be around 10 μA for a complete system on chip including voltage reference, regulators, wakeup blocks etc. [7].

With the increasing advent of high-speed mixed-signal and radio frequency (RF) devices, the automotive industry also sets high requirements for very low electromagnetic emission (EME) and high immunity to electromagnetic interference (EMI). This aggressive EMI can easily couple from an application ambient to the IC via cable harness or printed circuit board (PCB) tracks [9].

From the above-mentioned requirements, we selected the following criteria for the analysis of the basic bandgap cores: temperature drift over a wide temperature range from –50°C to 200°C, line regulation for supply voltage from 2 V to 4 V, and low EMC susceptibility over a wide high frequency (HF) range from 100 kHz to 1 GHz.

The rest of this paper is organized as follows. The integrated basic bandgap voltage reference core topologies are described in Sec. 2. The bipolar junction transistor collector leakage current compensation is described in Sec. 3, including investigated bandgap cores, used operational amplifier (OPA) model and whole simulation setup. Section 4 presents simulation results of output voltage temperature drift, sensitivity to the OPA input offset, line regulation, noise, mismatch, and EMC susceptibility. Finally, concluding remarks are outlined in Sec. 5.

2. Integrated Basic Bandgap Voltage Reference Topologies

The basic principle of creating temperature stable bandgap voltage is summing of two voltages, one with negative and one with positive temperature coefficient (marked as complementary to absolute temperature - CTAT and proportional to absolute temperature - PTAT) [10]. The CTAT voltage, which has negative TC, is equal to base-emitter voltage V_{BE} of a bipolar junction transistor (BJT) and the PTAT voltage, which has positive TC, is equal to a multiple of a base-emitter voltage difference

DOI: 10.13164/re.2022.0413

ΔV_{BE} between two BJTs with different collector current densities [10]. MOS transistors in a sub-threshold region can be used instead of BJTs but are usually not used in automotive bandgap designs due to their weakness in noise immunity [7]. To be able to compare bandgap core topologies and not BJT properties we use only NPN bandgap cores in this study.

There are several well-known basic topologies of bandgap voltage reference cores. The first chosen one is the Kuijk bandgap core [10]. This core is shown in Fig. 1.

Kuijk core usually employs two bipolar transistors Q1 and Q2 with the same currents I_1 and I_2 [4]. This means that the resistors R_1 and R_2 have the same value and a ratio n : 1 of bipolar transistor emitter areas A_{E1}/A_{E2} (also as the bipolar transistor units' ratio) is in most cases 8 : 1 in order to get a common centroid layout with Q2 in the middle. In a case of ideal BJTs without base currents, the output reference voltage is described by the following equation

$$V_{REF} = mV_T \ln\left(\frac{I_2}{I_1}n\right)\left(\frac{R_1}{R_3}+1\right)+V_{BE1} \tag{1}$$

where m is an emission coefficient with a value between 1 to 2, V_T is a temperature voltage $kT_{Junction}/q$ and V_{BE1} is the base-emitter voltage of the Q1 BJT.

The second chosen topology is the Brokaw bandgap core [10]. This core is shown in Fig. 2.

Brokaw core employs two BJTs Q1 and Q2 with the same collector currents I_{C1} and I_{C2} similar to the Kuijk bandgap core. In case of ideal BJTs without base currents I_B, the output reference voltage is described by the following equation

$$V_{REF} = V_{BE2} + \frac{R_4}{R_3}mV_T \ln\left(\frac{I_{C2}}{I_{C1}}n\right)\left(1+\frac{R_1}{R_2}\right). \tag{2}$$

Finally, the third chosen topology is the Tsividis bandgap core [11]. This core is shown in Fig. 3.

Tsividis core employs two BJTs Q1 and Q2 with the same emitter currents I_{E1} and I_{E2}. This means that the resistors R_1 and R_2 have the same value and the ratio n : 1 of bipolar transistor emitter areas A_{E1}/A_{E2} is in most cases 8 : 1. In the case of ideal BJTs without base currents I_B, the

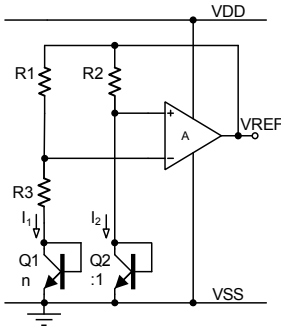

Fig. 1. The basic Kuijk bandgap core topology [10].

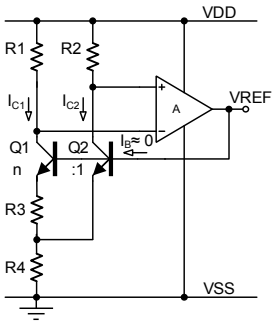

Fig. 2. The basic Brokaw bandgap core topology [10].

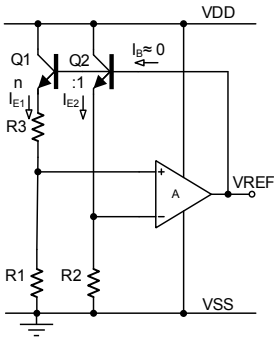

Fig. 3. The basic Tsividis bandgap core topology [11].

output reference voltage is described by the following equation

$$V_{REF} = V_{BE1} + mV_T \ln\left(\frac{I_{E2}}{I_{E1}}n\right)\left(1+\frac{R_1}{R_3}\right). \tag{3}$$

3. Investigations of the Bandgap Cores

The investigations of the selected bandgap cores include reference voltage temperature drift in the wide temperature range from –50°C to 200°C, sensitivity to the OPA input offset, line regulation, output noise, mismatch and EMC susceptibility analyzes. Firstly, we present two methods of collector leakage current compensations with proposed bandgap cores, an OPA simulation model and a common simulation setup. Finally, we describe achieved results and show comparison between proposed cores.

3.1 Collector Leakage Current Compensation

The collector of the vertical NPN type BJT is often isolated from the IC substrate only by a reverse polarized junction diode. The leakage current of this diode influences the accuracy of the bandgap especially when working with small collector currents (about 1 μA) at temperatures higher than 150°C [12].

Figure 4 shows a simplified cross section of a vertical NPN type BJT which is processed in a BCD technology. The leakage current of the BJT's collector diode D_{CQ} can cause error of the collector current. This effect mainly impacts Kuijk and Brokaw bandgap cores.

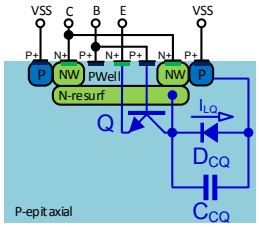

Fig. 4. The NPN BJT cross-section in IC.

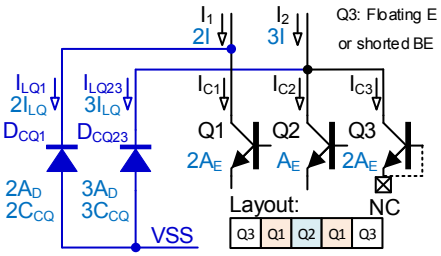

Fig. 5. The collector leakage current compensation principle.

Collector leakages can be compensated by adding $n-1$ dummy BJTs in parallel to Q2 in the case $I_{C1} = I_{C2}$ because we want to have the same ratio of leakage currents as the ratio of collector working currents [12]. This means adding seven BJTs when n is eight for well-known Brokaw 8 : 1 core. For this case, it is very difficult to reach full symmetry for 16 BJTs and the area is significantly increased. To reduce the area and have a symmetrical layout of the BJTs, we chose n equal to two and the collector currents I_{C1} and I_{C2} in the ratio of 2 : 3. The chosen BJT's ratio requires only two dummy BJTs connected in parallel to Q2 for the compensation of leakages as we used in [9]. Figure 5 shows the symmetrical layout of five BJTs in one row.

From the chosen ratio of collector currents 2 : 3 in the presented bandgap BJT configuration, the PTAT voltage as difference between two base-emitter voltages of Q2 and Q1 BJTs is simplified to the following form

$$\Delta V_{BE} = V_{BE2} - V_{BE1} = mV_T \ln\left(\frac{I_{C2}A_{E1}}{I_{C1}A_{E2}}\right), \tag{4}$$

$$\Delta V_{BE} = mV_T \ln\left(\frac{3I2A_E}{2IA_E}\right) \approx V_T. \tag{5}$$

This means no basic amplification of the temperature voltage. The BJT collector leakage currents compensation is described by the following equations where we assume collector current as a difference between input current and the BJT leakage current like for Q1: $I_{C1} = I_1 - I_{LQ1}$.

$$\Delta V_{BE} = mV_T \ln\left[\frac{\left(I_2 - I_{LQ23}\right)A_{E1}}{\left(I_1 - I_{LQ1}\right)A_{E2}}\right], \tag{6}$$

$$\Delta V_{BE} = mV_T \ln\left[\frac{3\left(I - I_{LQ}\right)2A_E}{2\left(I - I_{LQ}\right)A_E}\right] \approx V_T \tag{7}$$

where I is unit bias current and I_{LQ} is unit leakage current. The equations (6) and (7) show that the additional dummy BJTs add leakage currents in the required ratio and the collector currents ratio ideally stays the same. Therefore, the difference between the two base-emitter voltages is not impacted by the collector leakage currents.

3.2 Investigated Bandgap Cores

We propose nine simple bandgap cores from the three chosen basic bandgap core topologies with two methods of the collector leakage current compensation. We chose the compensation BJT Q3 (see Fig. 5) with a floating emitter [9] and a shorted base-emitter (BE) junction connected to emitter of Q2 [12] as two different versions for the leakage compensation. With the floating emitter, we expect mainly impact of the collector substrate junction leakage. With the shorted BE junction connected to emitter of Q2, we add leakage of closed bipolar to the circuit in emitters of BJTs. Figure 6 shows the proposed bandgap cores.

The chosen bandgap cores are:

a) Brokaw bandgap 2 : 1,
b) Brokaw bandgap 2 : 1 with the collector leakage current compensation where the compensation BJT has shorted BE junction,
c) Brokaw bandgap 2 : 1 with the collector leakage current compensation where the compensation BJT has floating emitter,
d) Self-supplied Brokaw bandgap 2 : 1,
e) Self-supplied Brokaw bandgap 2 : 1 with the collector leakage current compensation where the compensation BJT has shorted BE junction,
f) Self-supplied Brokaw bandgap 2 : 1 with the collector leakage current compensation where the compensation BJT has floating emitter,
g) Kuijk bandgap 2 : 1,
h) Kuijk bandgap 2 : 1 with the collector leakage current compensation where the compensation BJT has floating emitter and
i) Tsividis bandgap 2 : 1.

We also include well-known Brokaw 8 : 1 bandgap core as a reference. All proposed bandgap cores are designed to have the same operating point such as bias currents of the cores and the same ratio of currents and BJTs. The current consumption of each bandgap core is around 1.3 µA. We choose only one collector current compensation for the Kuijk bandgap core due to connection of the BJTs like diodes. Only BJT's intrinsic reverse polarized diodes between collectors and VSS ground keep collector leakage currents in the same ratio as the ratio of working currents $I_1 : I_2$ (Fig. 6 h)). In general, the Tsividis core doesn't need the leakage current compensation in collectors because it uses the emitter currents. Therefore, we firstly analyze this core without compensation transistors (Fig. 6 i)).

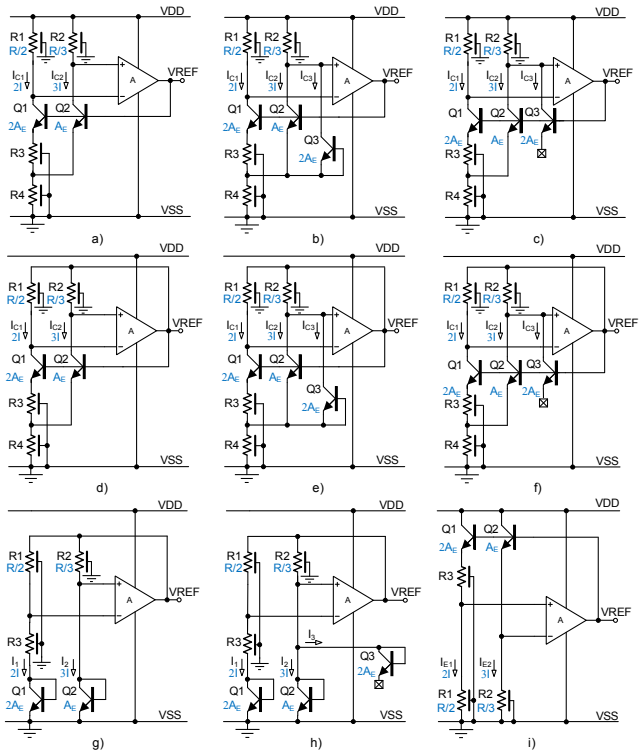

Fig. 6. The proposed bandgap cores for investigations.

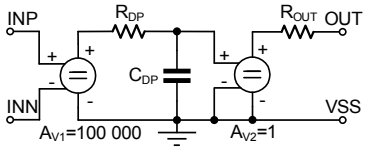

Fig. 7. The OPA circuit simulation model.

3.3 Operational Amplifier Model

To be able to investigate impact of the bandgap cores only, the operational amplifier is modeled by a simple idealized model with one frequency pole and an output resistance. The same OPA model (shown in Fig. 7) is used for each proposed bandgap.

The INP pin is a noninverting (positive) input and the INN pin is an inverting (negative) input of the OPA. The OPA consists of two voltage-controlled voltage sources (VCVSes) with a voltage gain A_V. Between these sources there is an RC network defining frequency of the dominant pole. The OPA simulation model has DC open loop gain 100 dB, dominant pole frequency 10 Hz, unity gain bandwidth 1 MHz and output resistance 1 kΩ. These chosen parameters are very close to a real bandgap OPA. The OPA model is independent of the supply voltage variations.

3.4 Simulation Setup

All proposed bandgap cores are analyzed one by one in the same simulation setup within the Cadence Virtuoso analog design environment. The common simulation setup schematic diagram is shown in Fig. 8.

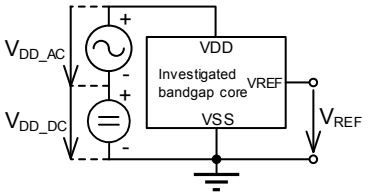

Fig. 8. The common simulation setup.

The V_{DD_DC} is 3 V as a common DC supply voltage source. The V_{DD_AC} is 0 V or 1 V peak with a sweeping frequency f as a common AC sine wave voltage source for EMC susceptibility investigations. We used analytical tools of the Cadence Spectre RF simulator for all simulations, especially an envelope analysis for the EMC susceptibility simulations.

4. Results

The simulation results include reference voltage temperature drift, sensitivity to the OPA input offset, line regulation, noise, mismatch, and EMC susceptibility which we analyzed for each proposed bandgap core.

4.1 Temperature Drifts

The overall reference voltage temperature drifts of all proposed bandgap cores were simulated for junction temperature from –50°C to 200°C. The reference voltage of each proposed bandgap core was normalized to the reference voltage at room temperature 27°C. The resulted overall temperature drifts are shown in Fig. 9.

From the overall temperature drifts, we can see that Kuijk 2 : 1 and Brokaw 8 : 1 cores have the highest sensitivity to unbalanced collector leakage currents. The mentioned collector leakage current effect is seen as higher voltage tail in the range from 150°C to 200°C. The self-supplied Brokaw 2 : 1 core has also high sensitivity to un-

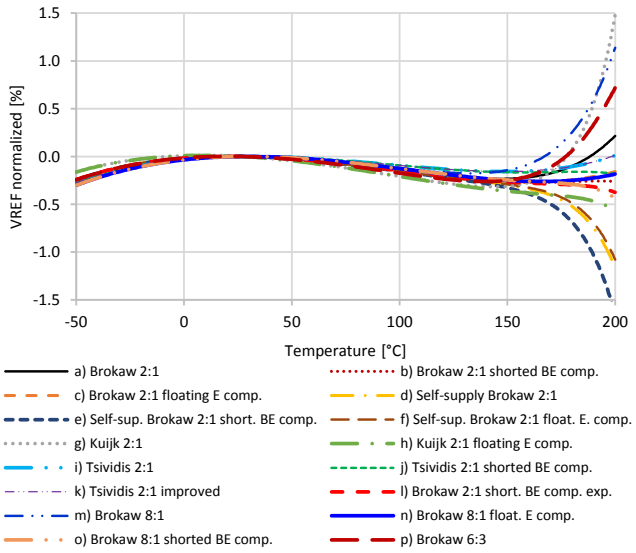

Fig. 9. The temperature drifts of all proposed cores.

balanced leakage currents and balancing of leakages does not help much due to saturation effect of BJTs. The saturation of BJTs is caused by voltage drops on the collector resistors. The increased voltages on the collector resistors push the BJTs to the unwanted deep saturation mode which results in decreasing of the reference voltage. The voltage drops on collector resistors cannot be very small because decreasing the voltage drop reduces the operating range at the OPA input and increases unwanted sensitivity to the OPA input offset.

The Brokaw 2 : 1 bandgap core has medium sensitivity to unbalanced leakage currents and balancing of collector leakage currents shows its essence for both leakage compensations. For compensation comparison and more investigation of each version, we prepare additional experimental leakage compensation setup with the shorted BE compensation BJT connected through a VCVS to the ground. This experimental connection cancels the influence on the resistive divider R3 and R4 and keeps leakage from collector to base/emitter (Fig. 10 l)). We tried to include the shorted BE leakage compensation in the Tsividis 2 : 1 bandgap core (Fig. 10 j)) and improved capacity balance at OPA inputs (Fig. 10 k)) in the same core as well. The resulting temperature drifts of Brokaw cores with different leakage compensations are shown in Fig. 11.

The leakage compensation for the Brokaw 2 : 1 core marked as Brokaw 2 : 1 short. BE comp. shows higher effect on the temperature drift than the version marked as Brokaw 2 : 1 float. E comp. due to higher effect of a collector-base (CB) junction leakage. The CB leakage in the shorted BE compensation version flows directly to the emitter due to the shorted BE junction. When we connect this emitter to the emitter voltage divider then the leakage influences the voltage ratio in the desired way resulting in a smaller temperature drift for temperatures above 150°C. We proved this effect by an experiment, where we decoupled the emitter of the compensation BJTs from the divider and maintained the same voltage conditions by the VCVS (Fig. 10 l)). The resulted temperate drift marked as Brokaw 2 : 1 short. BE comp. exp. (Fig. 11 l)) shows only one part of collector leakage compensation effect which is not sufficient. The experiment proved that the leakage also causes unwanted influence of voltages in the emitter circuit of the Brokaw bandgap core.

The CB leakage in the Brokaw 2:1 core with floating E compensation (see Fig. 6 f)) flows only to the base of the BJTs and impacts the voltage on positive input of the OPA. This compensation method shows a little bit temperature drift improvement, and we can say that it is not completely compensating the leakage effect. Both leakage compensation methods of the Brokaw 8 : 1 core also show their essence especially for compensation method marked as float. E comp. Nevertheless, this method significantly increases the layout area to 16 BJTs and they are very difficult to layout fully symmetrically.

We must point out that the proposed Tsividis 2 : 1 bandgap core has a little leakage current effect caused by unbalanced CB junction leakage currents. These currents flow into the emitter circuit through BJT bases and influence the PTAT voltage. This effect can be minimized by the shorted BE leakage compensation (Fig. 10 j)). The Tsividis 2 : 1 core has low temperature drift and even smaller drift with the proposed leakage compensation. The detailed temperature drifts of the Tsividis 2 : 1 bandgap core experiments are shown in Fig. 12.

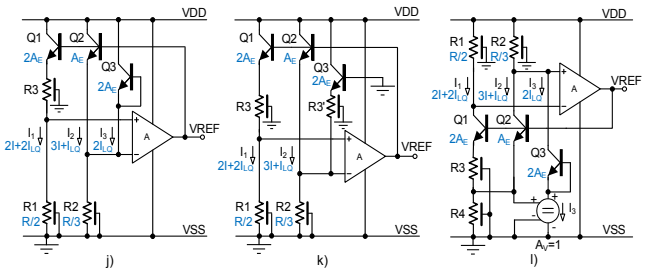

Fig. 10. Tsividis 2 : 1 j), k) and Brokaw 2 : 1 l) experiments.

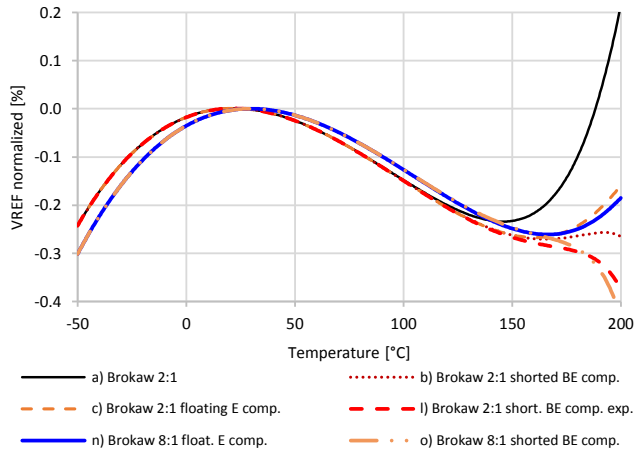

Fig. 11. Comparison of different leakage compensations.

4.2 Sensitivity to the OPA Input Offset

The reference voltage sensitivity to the OPA input offset is investigated by adding a voltage source in series to the OPA noninverting input. This voltage source models the input offset. We choose the input offset from 0 to 10 mV,

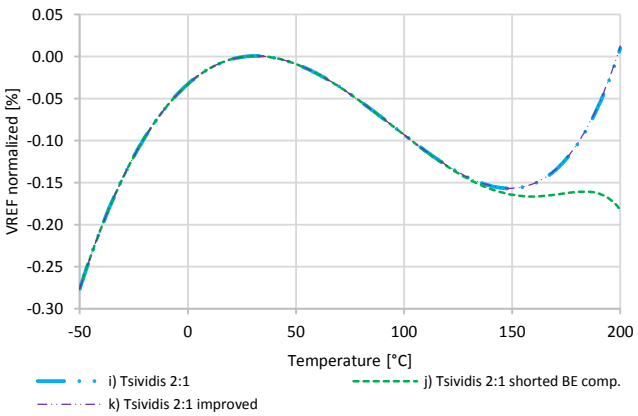

Fig. 12. The temperature drifts of Tsividis 2:1 cores.

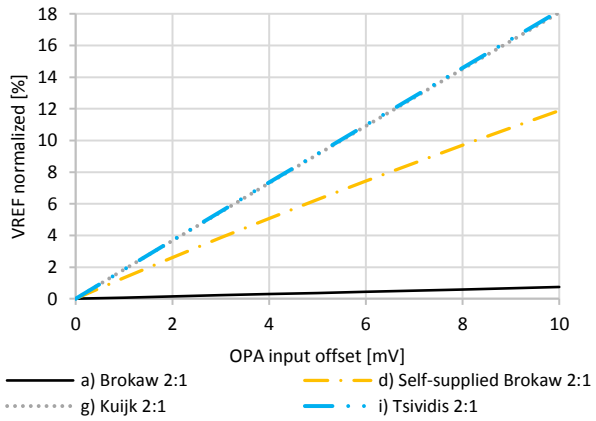

Fig. 13. The OPA input offset voltage sensitivity of the proposed bandgap cores at 27°C temperature.

close to real values. We analyzed the relative reference voltage sensitivities to the OPA input offset of proposed bandgap cores without leakage current compensations at room temperature 27°C. The resulted sensitivities are shown in Fig. 13.

The Kuijk and Tsividis cores show high sensitivity to the OPA input offset. This behavior is expected due to direct influence of the PTAT voltage. The self-supplied Brokaw 2 : 1 core shows medium sensitivity with a small nonlinearity caused by the saturation effect of the BJTs due to influenced voltage drops on collector resistors. For these bandgap cores an OPA offset cancellation technique is recommended like e.g., chopping [14]. The Brokaw 2 : 1 core has low sensitivity to the OPA input offset because the OPA offset influences only voltage on collector resistors, which define collector current ratio of the BJTs in the core.

4.3 Line Regulation

We simulated the supply line regulation of proposed bandgap cores with the OPA model from Sec. 3.3. We choose supply range from 2 V to 4 V, room temperature 27°C and we evaluated output voltages of each proposed bandgap core normalized to the reference values at 3 V. The resulted line regulations are shown in Fig. 14. When using real OPA, the resulted line regulations are worse, because here we see only bandgap core contributors.

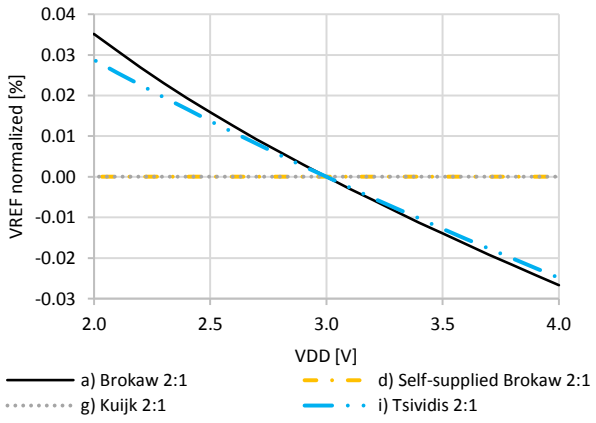

Fig. 14. Line regulations of VREFs at 27°C temperature.

4.4 The EMC Susceptibility

The EMC susceptibility simulation was performed as transient envelope analyzes with fifteen harmonics by Cadence Spectre RF simulator. The simulation results are post-processed after circuit settling for the VREF DC and the first harmonic for each selected bandgap core. We compared the Brokaw cores with both leakage current compensations and the Tsividis bandgap cores. The EMC susceptibility results as relative VREF DC voltage shifts are shown in Fig. 15.

The Brokaw 2 : 1 and 8 : 1 cores without leakage current compensation has medium EMC susceptibility due to unbalanced time constants defined by the collector resistors and BJT collector to VSS capacitances. When we use the leakage current compensation marked as float. E comp., the collector RC time constants are balanced for Brokaw cores. The leakage current compensation marked as shorted BE comp. shows also influence by the CB junction capacitance. While this version is good for temperature drift, for the EMC susceptibility causes slightly unbalanced collector time constants resulting in slightly higher voltage shift. Both leakage compensations show low rectification effect, which causes reference voltage shifts due to collector capacitances balancing at the OPA inputs. We see an effect of different collector resistors for Brokaw 2 : 1 with balanced BJT capacitors (Fig. 15 c)) in frequency range from 100 kHz to 10 MHz. This is caused by resistor's parasitic capacitance between its poly layer and well below, which is connected to VSS. The Tsividis 2 : 1 cores have high EMC susceptibility caused by the CB junction capacities. These capacities are effective at higher frequency than 1 MHz. These capacities together with the BJT capacities and emitter resistances create unbalanced RC networks, which are resulting in pass band rectification of the HF interference on the VDD supply. The Tsividis 2 : 1 improved core by approximately balanced RC networks shows better EMC

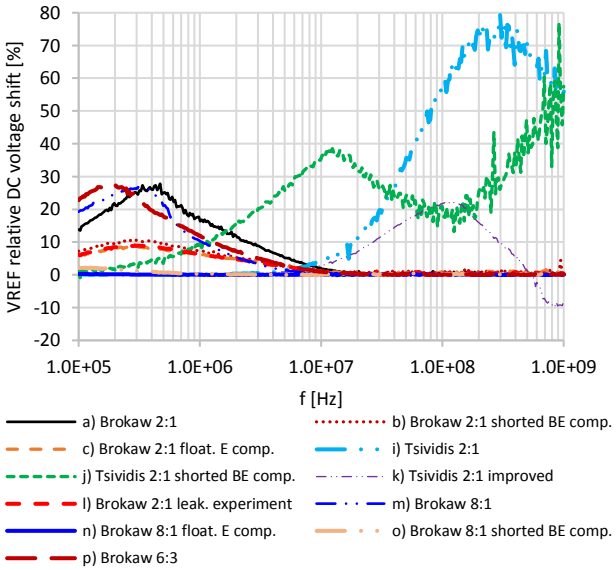

Fig. 15. Relative VREF DC voltage shifts of the selected bandgap cores induced by the 1 V peak sinusoidal HF EMI on the VDD supply with 3 V DC.

Proposed bandgap cores	Parameters							
	No. of BJTs [-]	TC [ppm/°C]	Sensitivity to OPA offset [%/mV]	Line regulation [%]	Voltage noise at 1 Hz [μV/√Hz]	Mismatch 6 sigma [mV]	DC shift induced by HF EMI on VDD, max. [%]	PSRR, min. [dB]
a) Brokaw 2:1	3	18.3	0.07	0.06	4.2	28.5	27.8	44.8
b) Brokaw 2:1, shorted BE comp.	5	10.9	0.07	0.06	4.2	28.5	10.6	77.7
c) Brokaw 2:1, floating E comp.	5	10.7	0.07	0.06	4.2	28.5	8.7	73.2
d) Self-supplied Brokaw 2:1	3	46.5	1.19	NA*	5.4	31.6	NA*	NA*
e) Self-sup. Brokaw 2:1, short. BE comp.	5	66.0	1.19	NA*	5.4	31.6	NA*	NA*
f) Self-sup. Brokaw 2:1, float. E comp.	5	43.2	1.19	NA*	5.4	31.6	NA*	NA*
g) Kuijk 2:1	3	71.8	1.81	NA*	5.6	27.1	NA*	NA*
h) Kuijk 2:1, float. E compensation	5	23.1	1.81	NA*	5.6	27.1	NA*	NA*
i) Tsividis 2:1	3	11.5	1.82	0.05	5.4	28.5	79.9	10.3
j) Tsividis 2:1, shorted BE comp.	5	11.1	1.82	0.05	5.4	28.5	76.8	9.8
k) Tsividis 2:1 with improvements	5	11.5	1.82	0.05	5.4	28.5	22.3	11.1
l) Brokaw 2:1 leakage experiment	5	15.1	0.07	0.06	4.2	28.5	9.0	78.3
m) Brokaw 8:1	9	57.5	0.05	0.06	3.3	15.7	26.7	38.3
n) Brokaw 8:1, float. E compensation	16	12.1	0.05	0.06	3.3	15.7	0.4	71.4
o) Brokaw 8:1, shorted BE comp.	16	17.4	0.05	0.06	3.3	15.7	2.2	77.5
p) Brokaw 6:3	9	39.1	0.08	0.06	3.1	18.2	27.3	45.4

Tab. 1. Comparison of proposed bandgap cores (NA* - Not available due to used ideal OPA model).

susceptibility as we expected. We also investigated a power supply rejection ratio (PSRR) of selected bandgap cores within EMC susceptibility analyzes. The reference voltage PSRR of each selected core is calculated from the first harmonic voltage amplitudes using the following equation

$$VREF\_PSRR = 10\log\left(\frac{\Delta V_{VDD}^2}{\Delta V_{ref}^2}\right) = 20\log\left(\frac{\Delta V_{VDD}}{\Delta V_{ref}}\right) \quad (8)$$

where ΔV_{VDD} is change of the VDD supply and ΔV_{ref} is change of the reference voltage. We consider the changes as first harmonic voltage amplitudes. The VREF PSRRs of selected bandgap cores are shown in Fig. 16.

The VREF PSRRs of the selected bandgap cores reflect behaviors of relative VREF DC voltage shifts. The unbalanced collector RC time constants of the Brokaw cores without leakage current compensation cause a small

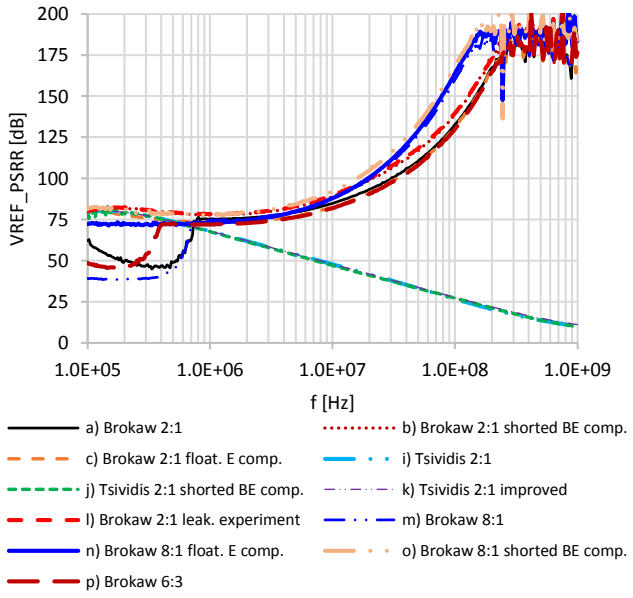

Fig. 16. The PSRR of the selected bandgap cores induced by the 1 V peak sinusoidal HF EMI.

OPA input differential voltage that is amplified by the OPA. This amplified AC voltage is added to the voltage reference resulting in lower PSRR. We noted that the OPA model has 1 MHz unity gain bandwidth. The leakage current compensation balances the collector RC time constants and results in higher PSRR in a frequency range from 100 kHz to 1 MHz. The Tsividis cores have low PSRR at higher frequencies above 1 MHz due to VDD coupling to the output through CB junction capacities. All investigation results of proposed bandgap cores are summarized in Tab. 1.

In the summary table of the proposed bandgap cores, there are temperature coefficients calculated from temperature drifts, relative sensitivities to OPA offset, relative line regulations in VDD range from 2 V to 4 V, output voltage noise, mismatch, and relative voltage DC shifts with PSRRs within EMC susceptibility analyzes.

We must note that the self-supplied Brokaw and Kuijk cores were supplied from an ideal OPA model,

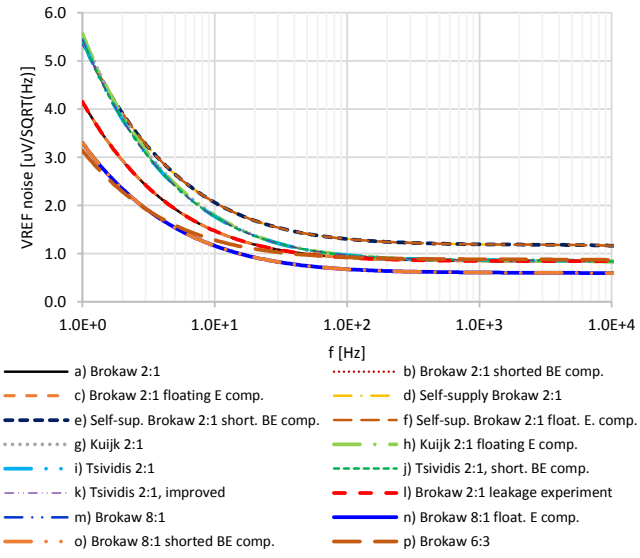

Fig. 17. The voltage noises of proposed bandgap cores.

which is not dependent on VDD supply like a real OPA. For this reason, the line regulation and EMC susceptibility with PSRR results are not included in this table because the results are dependent on parameters of the used OPA (see Fig. 7).

Figure 17 shows output voltage noises for each proposed bandgap core. The Brokaw 6 : 3 with Brokaw 8 : 1 have the lowest noise from proposed cores. The Brokaw 2 : 1 has medium noise. Kuijk 2 : 1 and Tsividis 2 : 1 have the highest output noise. The 1/f noise is given by collector current densities of BJTs. If we use higher count of BJTs in each branch of the core, the output 1/f noise is lower.

5. Conclusion

This paper presents comparative study of Kuijk, Brokaw and Tsividis integrated bandgap reference cores. The study includes comparison of two collector leakage current compensation methods and the leakage compensation for the Tsividis 2 : 1 core. On top of the EMC susceptibility comparison results, basic parameters like temperature drift, sensitivity to the OPA input offset, line regulation, output voltage noise and mismatch are presented and discussed. From the achieved results, the Brokaw 2 : 1 with floating E leakage compensation has low temperature coefficient 10.7 ppm/°C in the temperature range from –50°C to 200°C with further EMC susceptibility improvement possibility. The well-known Brokaw 8 : 1 core with the same compensation has a good matching and EMC susceptibility performance but it is paid by bigger area and not fully symmetrical layout of the BJTs.

Acknowledgments

The presented research was supported by the Internal Grant Agency of Brno University of Technology (the project no. FEKT-S-20-6526).

References

[1] KOK, C. W., TAM, W. S. *CMOS Voltage References: An Analytical and Practical Perspective.* Singapore: John Wiley and Sons, 2013. DOI: 10.1002/9781118275696

[2] HUIJSING, J., VAN DE PLASSCHE, R. J., SANSEN, W. M. C. (Eds.) *Analog Circuit Design, Low-Noise, Low-Power, Low-Voltage; Mixed-Mode Design with CAD Tools; Voltage, Current and Time References.* Springer, 1996, VIII, 422 p. DOI: 10.1007/978-1-4757-2462-2

[3] DUAN, Q., ROH, J. A 1.2-V 4.2-ppm/°C high-order curvature-compensated CMOS bandgap reference. *IEEE Transactions on Circuits and Systems*, 2015, vol. 62, no. 3, p. 662–670. DOI: 10.1109/TCSI.2014.2374832

[4] KANDADAI, H. Comparison of Kuijk and Brokaw voltage reference architectures for high precision on-chip references. *International Journal of Industrial Electronics and Electrical Engineering (IJIEEE)*, 2016, vol. 4, no. 8, p. 71–74. ISSN: 2347-6982. Available at: http://ijieee.org.in/

[5] SINGH, K. J., MEHRA, R., HANDE, V. Ultra low power, trimless and resistor-less bandgap voltage reference. In *Proceedings of 13th International Conference on Industrial and Information Systems (ICIIS)*. Rupnagar (India), 2018, p. 292–296. DOI: 10.1109/ICIINFS.2018.8721310

[6] HUANG, W., LIU, L., ZHU, Z. A sub-200nW all-in-one bandgap voltage and current reference without amplifiers. *IEEE Transactions on Circuits and Systems-II: Express Briefs*, 2021, vol. 68, no. 1, p. 121–125. DOI: 10.1109/TCSII.2020.3007195

[7] HARTL, P. An accurate voltage reference for automotive applications. *Electroscope*, 2014, no. 3, p. 1–5. ISSN: 1802-4564 Available at: http://electroscope.zcu.cz/

[8] OSMANOVIĆ, D., SKELEDŽIJA, I., ŠPOLJARIĆ, K., et al. Design of a tunable temperature coefficient voltage reference with low-dropout voltage regulator in 180-nm CMOS technology. In *Proceedings of 43rd International Convention on Information, Communication and Electronic Technology (MIPRO)*. Opatija (Croatia), 2020, p. 93–98. DOI: 10.23919/MIPRO48935.2020.9245163

[9] KROLÁK, D., PLOJHAR, J., HORSKÝ, P. An automotive low-power EMC robust Brokaw bandgap voltage reference. *IEEE Transactions on Electromagnetic Compatibility*, 2020, vol. 62, no. 5, p. 2277–2284. DOI: 10.1109/TEMC.2019.2958926

[10] RAZAVI, B. The bandgap reference [A circuit for all seasons]. *IEEE Solid-State Circuits Magazine*, 2016, vol. 8, no. 3, p. 9–12. DOI: 10.1109/MSSC.2016.2577978

[11] SANSEN, W. Bandgap and current reference circuits. *Analog Design Essentials*. *The International Series in Engineering and Computer Science,* 2006, vol. 859. Boston (MA): Springer. DOI: 10.1007/0-387-25747-0_16

[12] RADOIAS, L., ZEGHERU, C., BREZEANU, G. Substrate leakage current influence on bandgap voltage references in automotive applications. In *Proceedings of CAS 2012 (International Semiconductor Conference)*. Sinaia (Romania), 2012, p. 389–392. DOI: 10.1109/SMICND.2012.6400752

[13] YANG, S., MAK, P.-I., MARTINS, R. P. A 104μW EMI-resisting bandgap voltage reference achieving –20dB PSRR, and 5% DC shift under a 4dBm EMI level. In *Proceedings of 2014 IEEE Asia Pacific Conference on Circuits and Systems (APCCAS)*. Ishigaki (Japan), 2014, p. 57–60. DOI: 10.1109/APCCAS.2014.7032718

[14] MA, Y., BAI, CH., WANG, Y., et al. A low noise CMOS bandgap voltage reference using chopper stabilization technique. In *Proceedings of 5th International Conference on Integrated Circuits and Microsystems.* Nanjing (China), 2020, p. 184–187. DOI: 10.1109/ICICM50929.2020.9292198

About the Authors ...

David KROLÁK received his B.Sc. and M.Sc. degrees in Electronics and Communication from the Dept. of Radio Electronics, Brno University of Technology, Brno, Czech Republic, in 2014 and 2016, respectively. He is currently a student of a combined doctoral study in Electronics and Communications program of the same department. From 2016, he is working at ON Semiconductor and onsemi as an EMC engineer and analog designer. His research interests include an analog/mixed-signal IC design for automotive products and electrical measurements with focus on EMC at the IC level.

Pavel HORSKÝ received his M.Sc. degree in Radio Electronics and the Ph.D. degree in the field of metrology from the Brno University of Technology, Brno, Czech

Republic, in 1994 and 1998, respectively. In 2011, he became an Associated Professor at the same university. He is teaching analog design courses for Ph.D. students. From 1997, he was an analog and mixed-signal design engineer, technical project leader and leader of analog design group at Alcatel Microelectronics, AMI Semiconductor and ON Semiconductor and onsemi. He is currently a member of technical staff with onsemi. He has authored and coauthored more than 60 publications and 25 issued US patents. His professional interests include an analog/mixed-signal IC design for automotive products with focus on EMC, ESD and reliability.